Striking Influence of the Catalyst Support and Its Acid–Base Properties: New Insight into the Growth Mechanism of Carbon Nanotubes

Arnaud Magrez,[†,‡,*] Rita Smajda,[†] Jin Won Seo,[†,§] Endre Horváth,[†] Primož Rebernik Ribič,[⊥] Juan Carlos Andresen,[∥] Donatello Acquaviva,[¶] Areta Olariu,[†] Gábor Laurenczy,[#] and László Forró[†]

[†]Laboratory of Complex Matter Physics and [‡]Centre for Research on Electronically Advanced Matter, Ecole Polytechnique Fédérale de Lausanne, Switzerland, [§]Department Metallurgy and Materials Engineering, Katholieke Universiteit Leuven, Belgium, [⊥]Laboratory of Physics of X-rays, Ecole Polytechnique Fédérale de Lausanne, Switzerland, [∥]Institute for Theoretical Physics, Swiss Federal Institute of Technology Zurich, Switzerland, and [¶]Nanoelectronic Devices Group (NANOLAB) and [#]Laboratory of Organometallic and Medicinal Chemistry, Ecole Polytechnique Fédérale de Lausanne, Switzerland

ABSTRACT In the accepted mechanisms of carbon nanotube (CNT) growth by catalytic chemical vapor deposition (CCVD), the catalyst support is falsely considered as a passive material whose only role is to prevent catalytic particles from coarsening. The chemical changes that occur to the carbon source molecules on the surface are mainly overlooked. Here, we demonstrate the strong influence of the support on the growth of CNTs and show that it can be tuned by controlling the acid–base character of the support surface. This finding largely clarifies the CCVD growth mechanism. The CNTs' growth stems from the support where the presence of basic sites catalyzes the aromatization and reduces the complexity of CNT precursor molecules. On basic supports, the growth is activated and CNTs are more than 1000 times longer than those produced on acidic supports. These results could be the bedrock of future development of more efficient growth of CNTs on surfaces of functional materials. Finally, the modification of the aciditiy of the catalyst support during the super growth process is also discussed.

KEYWORDS: amphoteric · Al_2O_3 · TiO_2 · Brønsted · oxidative dehydrogenation · water

Recent outstanding progress in the growth of carbon nanotubes (CNTs) have confirmed the catalytic chemical vapor deposition (CCVD) process as a viable method for large-scale and low-cost production of CNTs with controlled morphological, physical, and chemical properties.[1−4] The advances in *in situ* characterization techniques allow a real-time observation of CNT growth, providing new insights into the generally accepted dissociation–diffusion–precipitation mechanism over supported catalytic nanoparticles.[5] In this mechanism, the carbon source is first dissociated by nanoparticles which subsequently dissolve the carbon produced by the dissociation reaction, and once supersaturated, carbon precipitates from the nanoparticles to form CNTs. However, there are several growth experiments that are difficult to explain with the concepts of the dissociation–diffusion–precipitation mechanism. For example, CNTs have been successfully grown from semiconductor nanoparticles that do not catalyze carbon,[6] from metal,[7,8] or oxide particles which do not dissolve carbon.[9−11] Even using conventional Fe-, Ni-, and Co-based nanoparticles, unexpected behaviors have also been observed. Pregrowth catalyst activation treatment,[12] or the use of the C deposition route based on oxidative dehydrogenation chemistry,[13,14] enables a dramatic reduction of the CNT growth temperature. The addition of nitrogen,[15] or oxygen-containing species,[16−18] to the carbon source enhances the catalyst activity. Growth rates are dramatically improved, and subcentimeter carpets containing vertically aligned CNTs are obtained within a few minutes.[13,16] These features are very important, and they need explication. In general, the role of the surface of the nanoparticle support during the growth of CNTs is considered to be marginal. However, although the range of materials used as nanoparticles is expanding, the number of supports yielding high-quality CNT growth remains limited.[19] This indicates that the role of the support could be as important as that of the nanoparticles and is not only restricted to the limitation of nanoparticle coarsening. Thus, a new mechanism has to be proposed which takes into account that nanoparticle supports actively participate in the growth of CNTs.

An alternative growth mechanism based on the self-assembly of acetylene into polyaromatic fragments has recently been

* Address correspondence to arnaud.magrez@epfl.ch.

Received for review January 3, 2011 and accepted April 25, 2011.

Published online April 25, 2011
10.1021/nn200012z

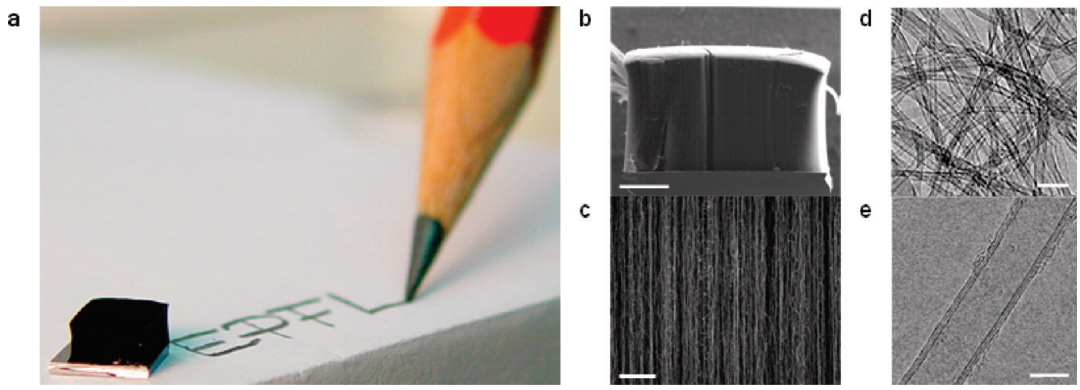

Figure 1. A 2.5 mm thick carpet of CNTs produced from ethylene at 750 °C over Fe_2Co nanoparticles supported by basic alumina surface. SEM micrographs of the carpet show that CNTs are well-aligned (b,c). From the mass of the carpet and the dimensions of CNTs, the density is estimated to be about 10^{11} CNTs per cm^2. TEM micrographs reveal CNTs to have, for the most part, 2−3 walls and high structural quality with clean surface (d,e) Scale bars are (b) 1 mm, (c) 1 μm, (d) 20 nm, and (e) 4 nm.

proposed for the growth of CNTs by CCVD. In this "polymerization"-like model, the CNT growth proceeds by the addition of new small polyines or graphene-like fragments built from unsaturated molecules to the growing CNTs. A CNT itself catalyzes the reaction while it undergoes growth. Although the model fits well with the experimental kinetics data for the growth of vertically aligned CNTs,[20,21] and it is substantiated by some theoretical studies,[22] the role of the support has not been considered.

In this article, we report on the activation of the surface of the nanoparticle support for the growth of CNTs by a simple and very efficient chemical treatment which changes its acid−base properties. These results clearly demonstrate the strong influence of the acid−base character of the support surface on the growth of CNTs, similar to all catalytic petrochemical processes.[23] When the support surface is made basic or when the acidity of the support is modified from Lewis to Brønsted by water molecules during the CCVD process, millimeter thick carpets of CNTs are produced in a few minutes. Additional expensive and demanding pregrowth treatments by physical means are unnecessary in order to activate the nanoparticles and enhance the CNT growth rate. Besides the technological relevance of this study, it is the first time that the role of the nanoparticle support during the growth of CNTs by CCVD has been clearly identified. On the basis of these results, we give a clear mechanism for the CCVD growth of CNTs and go beyond the usual "empirical recipe" approach. In our model, the surface properties of the support control the selectivity of the catalyst in order to enhance the growth of CNTs. The growth is initiated on the substrate where ethylene undergoes reactions in which intermediate fragments (larger hydrocarbons) are produced. While these intermediate fragments diffuse toward the nanoparticles, their size and their degree of saturation, branching and aromatization are regulated by the acid−base properties of the support. Once on the nanoparticle surface, the dehydrogenation and cyclic dehydrogenation of the intermediate fragments are completed while they incorporate the CNT structure. This new mechanism sheds new light on the role of water in the supergrowth CVD process.[16,24,25]

RESULTS AND DISCUSSION

Figure 1 demonstrates a representative carpet of CNTs produced at 750 °C from ethylene over Fe_2Co nanoparticles supported by an Al_2O_3 buffer layer grown on Si. Prior to the growth, the catalyst was treated by an ammonium hydroxide solution to enhance the basic character of the Al_2O_3 surface. Carpet based on aligned CNTs of a thickness as high as 2.5 mm can be obtained in 30 min. Typically, CNTs grown from a 0.5−1 nm thick film of metal reveal a mixture of single-, double- and triple-walled CNTs.

It is interesting to note that most of the carpets with millimeter thicknesses have exclusively been produced when alumina is used as a support.[26] Alumina is indeed an amphoteric material whose surface can exhibit acidic or basic properties depending on its synthesis or deposition process as well as on the conditions of post-synthetic chemical treatment. To modify the acid−base properties of the support after its deposition by e-beam evaporation on Si wafer, the catalyst (including the nanoparticles and the support) is immersed in a solution with a controlled pH. The pH is adjusted from 4 to 12 by adding HCl or NH_4OH to reinforce the acidic or basic character of the alumina layer, respectively. The acid−base properties of the surface were confirmed by the FTIR measurements of pyridine and CO_2 adsorption (see Supporting Information). As shown in Figure 2, the thickness of CNT carpets strongly depends on the pH of the solution used to treat the catalyst. Furthermore, the ethylene flux influences the length of the CNTs and their structural quality (Figure 2b,c). A maximum thickness of 1.35 mm is reached using Fe nanoparticles

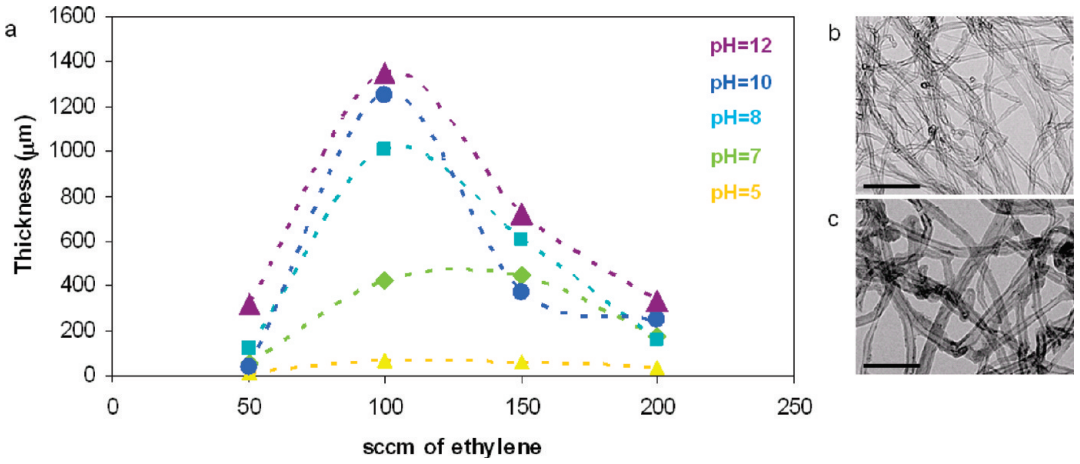

Figure 2. Evolution of the CNT carpet thickness as a function of the ethylene flux and the conditions of the chemical treatment of the catalyst including nanoparticles and support (a). TEM micrographs of CNTs were produced at 750 °C over Fe particles on alumina layer using ethylene flux lower or equal to 100 sccm (b) and higher than 100 sccm (c). The scale bar is 50 nm. For an ethylene flux lower or equal to 100 sccm, high-quality CNTs with a clean surface were obtained. For higher ethylene fluxes, heavy carbon deposition proceeds simultaneously to the growth of CNTs, leading to early catalyst poisoning, and the carpet thickness is reduced. Large quantity of amorphous carbon can be found on the surface of CNTs (see also HRTEM micrographs in Supporting Information).

when ethylene is introduced with a flux of 100 sccm over a catalyst treated with a pH = 12 solution. For the same ethylene flux, the carpet thickness is more than 1000 times lower for a chemical treatment with a pH = 4 solution. These results clearly illustrate the effect of the acid−base properties of the support surface on the yield of the CNT growth. The chemical process for activation described in this study is a controllable and reproducible method, significantly less demanding than activation by plasma or laser treatment.[1]

The steady increase of the growth rate with increasing ethylene flux up to 100 sccm means that all of the carbon atoms are incorporated into the CNTs. Above this flux, heavy amorphous carbon deposition occurs on the CNT surface as well as on the nanoparticles and the support, slowing the CNT growth kinetic.

The evolution of the carpet thickness is plotted as a function of the chemical treatment conditions "pH" for 100 sccm ethylene flux in Figure 3a. For CNTs grown over Fe supported by alumina, the transition from a thin to thick carpet occurs very abruptly. The change of the pH of the solution from 6 to 8 results in an increase of the carpet thickness by more than 1 mm. These facts clearly demonstrate the key role of the support in the CNT growth by CCVD. The pH of the inflection point of the curve is close to 7.5. This value falls into the range of the isoelectric point (number of Lewis basic sites is balanced by the number of Lewis acidic sites: $n_{\text{Lewis base}}/n_{\text{Lewis acid}} = 1$) conventionally measured for alumina materials.[27] When the balance is modified by a high pH chemical treatment ($n_{\text{Lewis base}}/n_{\text{Lewis acid}} > 1$), the thickness of the CNT carpet increases up to 1.35 and 2.5 mm when nanoparticles are composed of Fe and Fe_2Co, respectively. The inner diameter, which is directly correlated with the nanoparticle diameter, remains unchanged when the pH of the chemical treatement is raised from 4 to 12 (Figure 3c and confirmed by ESR in Supporting Information). However, the pH change influences the outer diameter, thus the number of walls as well as the length of the CNTs (Figure 3d) depends on the applied pH value. These evolutions are in agreement with the increased yield of the reaction up to about 10^6 mol of C as CNTs per mol of Fe_2Co for a support with basic character. In contrast, the chemical treatment with a low pH solution yielding a surface $n_{\text{Lewis base}}/n_{\text{Lewis acid}}$ ratio lower than 1 dramatically reduces the yield of the reaction and the length of the CNTs by more than 2 orders of magnitude, down to 20 μm short CNTs. Using TiO_2 instead of Al_2O_3 as support, similar dependence of the carpet thickness is observed as a function of the pH of the solution used for catalyst activation (Figure 3a). However, the pH of the inflection point is reduced to about 6.3. This is consistent with the lower isoelectric point values commonly measured for TiO_2 as compared to that of Al_2O_3.[27] In addition, the maximum thickness obtained for TiO_2-based catalyst is limited to 46 μm (Figure 3a). This difference in the maximum thicknesses of CNT carpets is attributed to the strength of the basic sites, as shown by the lower Hammett constant of TiO_2 as compared to the constant of Al_2O_3 materials.[23]

Similar dependence of the carpet thickness on pH is obtained when CNT growth proceeds from an equimolar mixture of acetylene and CO_2 by an oxidative dehydrogenation reaction (Figure 3b).[13] Despite the difference in the chemical reaction producing CNTs, the strong dependence of the growth on the basic and acidic sites of the support surface is confirmed. Furthermore, the growth over Fe and Fe_2Co nanoparticles

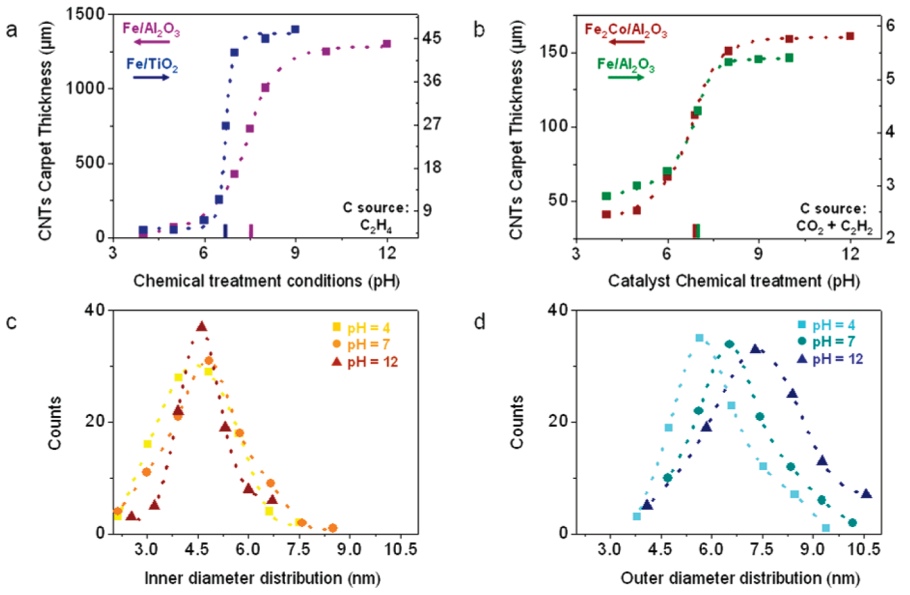

Figure 3. Evolution of the CNT carpet thickness as a function of the pH of the solution used to treat the catalyst. (a) Growth was performed at 750 °C using ethylene over Fe nanoparticles deposited on Al_2O_3 (pink) and TiO_2 (blue). (b) Growth by oxidative dehydrogenation chemistry from an equimolar mixture of acetylene and CO_2 at 750 °C over Fe_2Co (red) and Fe (green) supported by alumina. The arrows indicate the corresponding ordinate. The ticks indicate the pH corresponding to the inflection point (known as isoelectric point). Inner (c) and outer (d) diameter distribution of CNTs produced over Fe particles supported by Al_2O_3 treated at pH = 4 (square), pH = 7 (circle), and pH = 12 (triangle). The distribution was obtained by measuring diameters of 100 CNTs per sample. The composition, the particle size, as well as the roughness of the catalyst after chemical treatment and heat treatment under Ar and H_2 were analyzed by electron spin resonance (ESR), atomic force microscopy (AFM), transmission electron microscopy (TEM), and X-ray photoelectron spectroscopy (XPS). These characterizations of the nanoparticles and Al_2O_3 confirmed that neither of them had been etched during the chemical treatment (see Supporting Information). The inner diameter distribution of the CNTs, proportional to the nanoparticle diameter, is independent of the chemical treatment conditions. The support roughness remains constant for pH ranging from 4 to 12 (see Supporting Information). The composition and the surface area of the catalyst do not change with the pH adjustment and cannot explain the strong pH dependence of the CNT carpet thickness.

shows that the pH of the inflection points is identical in both cases, meaning that the chemical treatment affects mostly the properties of the alumina (Figure 3b). The maximum thickness of CNT carpets achieved on Al_2O_3 is lower than that in conventional growth experiments from ethylene (Figure 3a) since the carbon source molecules are introduced in the reactor at lower flux. As an alternative to Al_2O_3, CaO might be an effective nanoparticle support since it has a higher Hammett constant than Al_2O_3. It has been shown recently that, as a support, it yields 4 mm thick mat of CNTs.[13]

All of the experimental data reported here corroborate that the growth of CNTs depends on the surface properties of the nanoparticle support. This implies that the dissociation–diffusion–precipitation mechanism has to be modified in order to take into account the role of the support with the hydrocarbon chemistry at the surface. The properties of the surface influence the selectivity of the catalyst between polymerization, isomerization, and dehydrogenation reactions undergone by the hydrocarbon molecules adsorbed on the support. The degree of unsaturation, branching, and aromatization of the hydrocarbon molecules produced by such reactions is therefore dependent on the acid–base properties of the surface of the support. The high and low yield pathways are sketched in Figure 4.

The proposed scenario for the base-catalyzed reactions of ethylene is in line with the polymerization-like mechanism suggested by other groups.[20,34] It involves, as the first step, the formation of a carbanion. The stability of the carbanion increases with decreasing number of alkyl groups bonded to the negatively charged carbon. Consequently, carbanions undergo skeletal rearrangement, leading to a drastic reduction of the structure branching of the hydrocarbon adsorbed on basic supports (R_1 base). The addition to the adsorbed hydrocarbon of further molecules from the gas phase proceeds by increasing the length of the chain of the linear hydrocarbon similarly to polymerization process (R_2 base).[28] However, as polymerization of unsaturated hydrocarbons is limited on basic catalysts, the process results in short oligomers. These linear molecules undergo subsequent dehydrogenation and cyclization to alkylaromatic hydrocarbons when their length exceeds six carbon atoms (R_3 base).[29] The following base-catalyzed reaction of alkylaromatic molecules with subsequent hydrocarbons results exclusively in the enlargement of the alkyl group attached to the aromatic ring (R_4 base).[30] Once the alkyl groups are long enough, hexagonal rings close

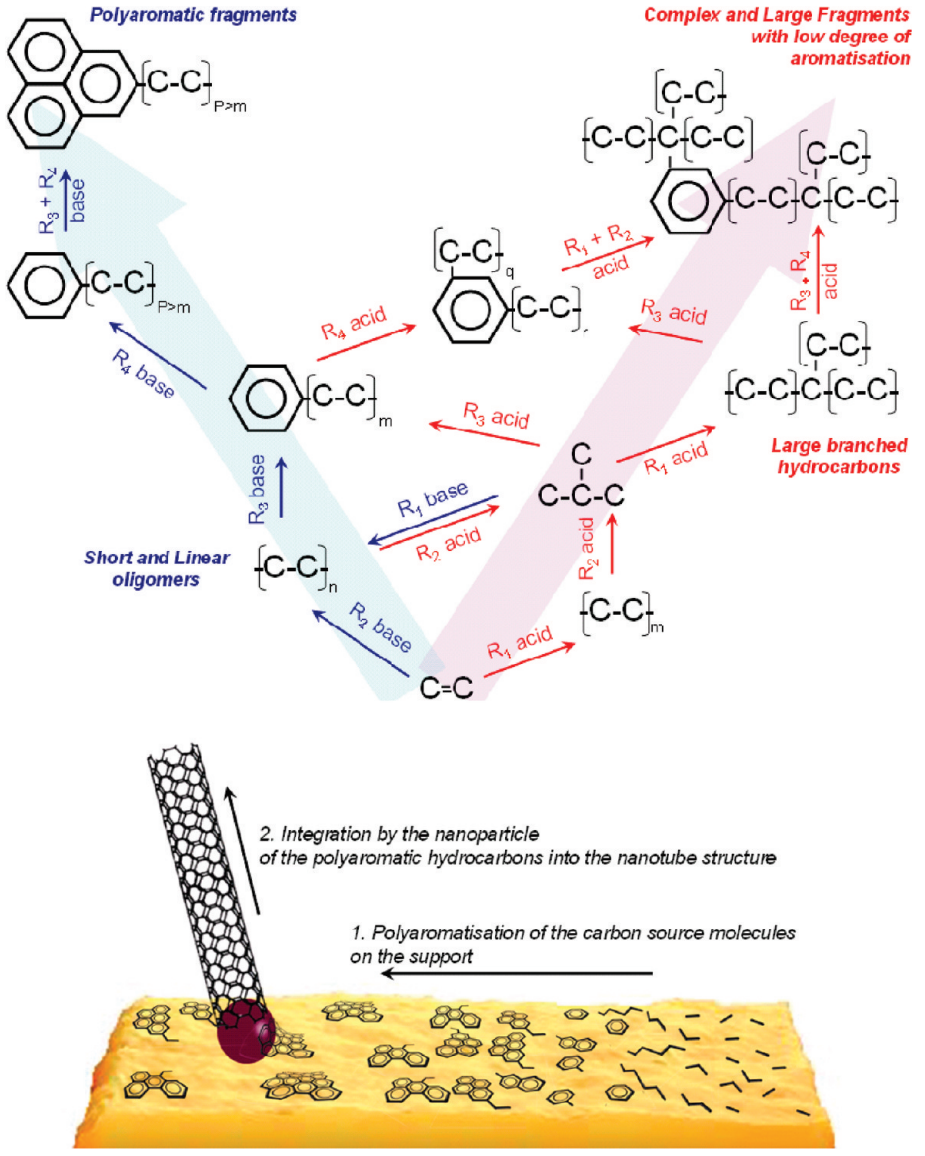

Figure 4. (Top) Chemical mechanism undergone by the hydrocarbons adsorbed on the surface of the supports. The shaded arrows in the background illustrate the overall chemical mechanism undergone by ethylene over the support with basic (blue) and acidic (red) properties. It has to be noted that ethylene undergoes limited oligomerization in the gas phase prior to the adsorption on the support. This results in small size polymers typically with a low number of carbon atoms, as evidenced by mass spectroscopy.[33] They are linear and have a variable degree of unsaturation. On basic alumina, the skeletal rearrangement of these oligomers preserves their linear shape. They undergo facile aromatization by the R_3 base reaction if they contain more than 6 carbon atoms after polymerization. In this scheme, hydrogen has been omitted for clarity so C−C includes the unsaturated C−C bond, as well. (Bottom) Scheme illustrating the new growth mechanism of CNTs by CCVD based on a two-step process. At first, carbon source molecules produce polyaromatic intermediate fragments on the support. The size and the structure of the fragments is controlled by the surface properties of the support. Second, the fragments are integrated into the CNT structure by the nanoparticles.

and dehydrogenate (R_3 base) to produce a new aromatic ring attached to the previous ring, resulting in polyaromatic molecules (R_5 base). Ultimately, polyaromatic fragments could be formed by repeated aromatic ring addition. The sequence of reactions describes an ideal picture of the chemical mechanism applied to basic substrates. It requires the production of highly aromatic fragments with low branching and limited size, which is favorable on basic support. Highly branched fragments can be incorporated into the CNT cylinders but will very likely results defective structures.

As can be seen in Figure 5, discontinuous wall pieces consisting of graphitic fragments not integrated in the CNT structure can be found in the high-resolution TEM micrographs at the CNT surface as well as inside CNTs. It is likely that these fragments also contribute to the D band of the Raman spectrum (see Supporting Information) and could support the existence of polyaromatic intermediate species catalyzed by basic supports forming the building blocks for CNT structures.

When alumina contains Lewis acidic sites on its surface, the growth of CNTs is dramatically limited.

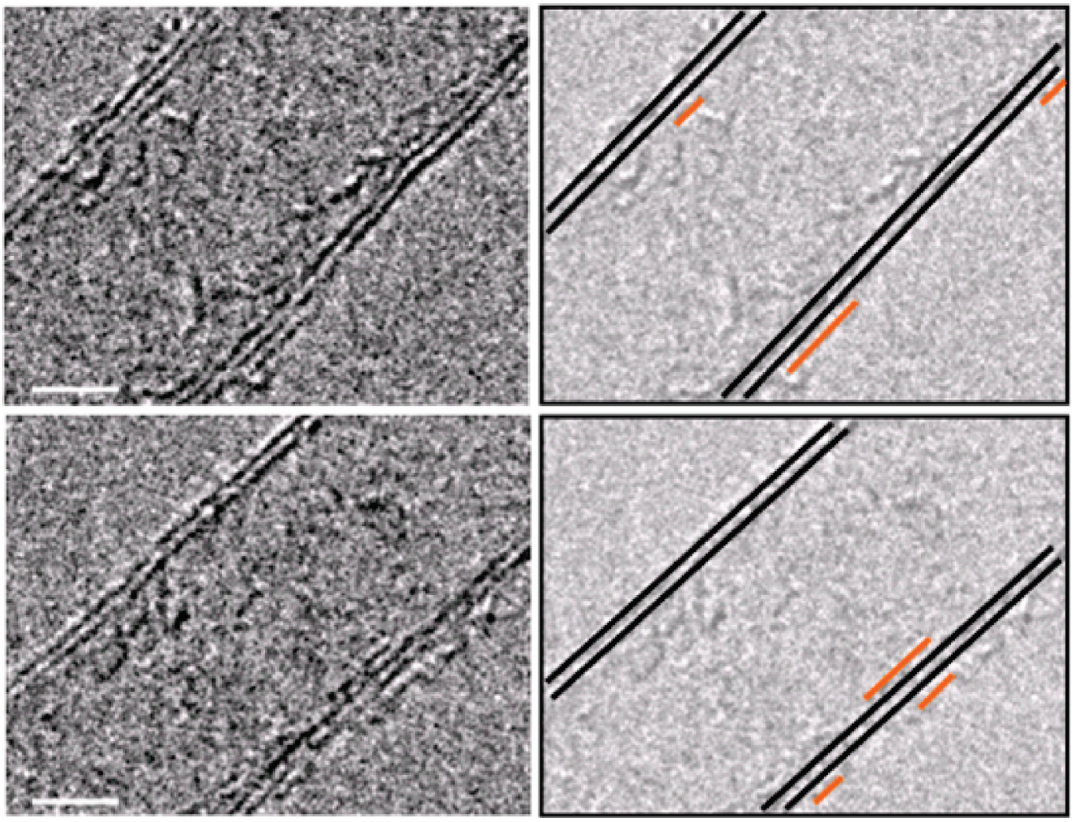

Figure 5. HRTEM micrographs showing the presence of polyaromatic fragments at the inner and outer walls of the CNTs (left panels). The size of fragments varies from 1 to 3 nm corresponding to molecules containing 20 to 200 aromatic rings, respectively, if the fragments are assumed to have isotropic structure. The CNT walls and graphitic fragments are, respectively, highlighted as black and orange lines for clarity (right panels). The distance between the fragments and the CNT wall is similar to the inter tube distance conventionally measured in MWCNTs (see Supporting Information). The scale bar is 2 nm.

Acidic oxides (including alumina materials) are recognized as efficient catalysts for the polymerization of unsaturated hydrocarbon (R_1 acid). This is testified by the very large number of processes developed in the olefin industry on the basis of acidic catalysis since the beginning of the 20th century.[31] When long chain hydrocarbons are adsorbed on Lewis acidic sites, they form carbocations. As opposed to the carbanion, the stability of the carbocation increases with the number of alkyl groups attached to the positive charge bearing carbon. This explains the capacity of acidic catalysts to cause isomerization of hydrocarbons. In particular, fast skeletal rearrangement leads to complex molecules with a branched structure (R_2 acid). These hydrocarbons undergo a limited dehydrogenation and aromatization over acidic alumina (R_3 acid) as compared to the basic counterparts.[29] Moreover, the acid-catalyzed reactions of aromatic molecules with ethylene allow the addition of alkyl groups to the aromatic ring and further increase the complexity of the hydrocarbon structure (R_4 acid).[30] As a product of these reactions, which are completely different from the base-catalyzed reactions, large molecules of unsaturated hydrocarbons with a complex structure are generated on the surface of the alumina. They have difficulty diffusing to the nanoparticles to be integrated into CNTs *via* cyclic dehydrogenation.

The drastic difference between the hydrocarbon structure produced over acidic and basic supports gives an explanation of the CNT growth rates measured (Figure 3a and Supporting Information). Hydrocarbons with a high degree of aromatization and low complexity produced on basic supports are better precursors for building CNTs than large and branched precursors produced on acidic supports. Conversely, unsaturated hydrocarbon precursors formed on the support, which are rich in electrons, may act as organic bases and neutralize the acidic sites. This rapidly renders the catalyst inactive and limits the yield of the reaction, which results in CNTs with reduced lengths, as shown in Figure 3a,b. However, the graphitic structure of the CNTs produced over supports treated with low and high pH solutions is very similar, as revealed by Raman scattering spectroscopy (Supporting Information). An intense 2D band in the Raman spectra confirms CNTs to be high-quality materials with low defect density regardless of the surface properties of the support.[32] Consequently, Fe-based nanoparticles are efficient at modifying hydrocarbons into well-graphitized CNTs despite the characteristics

of the hydrocarbon structure formed on the support. However, the kinetics of such a modification (reflected in the dependence of the length and diameter of the CNTs) is enhanced when hydrocarbons exhibit a higher degree of aromatization and lower complexity. As a consequence, the growth mechanism should be described in a two-step process where both nanoparticles and support are active (Figure 4). CNT growth is initiated on the support as illustrated by the dependence of the acid−base properties of its surface. First, ethylene molecules undergo reactions toward polyaromatic molecules on the support while diffusing toward the nanoparticles. The growth continues on the surface of the nanoparticles where precursor molecules assemble by dehydrogenation or cyclodehydrogenation reactions into CNTs. Finally, the diameter of the CNTs is controlled by the morphology and size of the nanoparticles.

The formation of intermediate hydrocarbon fragments acting as precursors for CNT structure in CCVD was mentioned, and a polymerization-like mechanism was suggested in recent studies, where thicker CNT carpets were obtained by using an upstream heat treatment of the ethylene source[33] or by mixing ethylene with alkynes.[34] However, the quality of the CNTs is reduced as the heat treatment temperature of ethylene is raised, which is necessary to increase the yield of the reaction. In our model, such a temperature increase causes a drastic enhancement of the kinetics of hydrocarbon modification in the gas phase and results in the formation of more complex intermediate fragments with poorly controllable size, degree of aromatization, and branching of their structure. The catalyst lifetime is shorter, the CNT length is limited, and the CNT structure is more defective when the same growth temperature is used.[35] Hence, the effect on the CNT growth induced by the upstream heat treatment of ethylene is less favorable than the adjustment of the basic character of the support surface. Consequently, the control of the surface properties of the catalyst support represents a unique method to select between reactions undergone by the carbon source in the reactor. Furthermore, the CCVD process is faster, and the quality of the CNT materials is higher when the catalyst is properly activated by chemical treatment.

The presence of water is known to enhance dramatically the CCVD process. Although it has been extensively studied, the role of water is not yet identified and just few hypotheses exist in the literature.[36,38] One of the suggestions is that water can etch amorphous carbon deposited onto the nanoparticles and preserve them from poisoning.[36] However, this proposition seems to be not consistent with the intense deposition of carbonaceous material on the CNT surface during the growth, which can react with water molecules, preventing them from reaching the catalyst nanoparticles for cleaning its surface.[37] However, nanoparticles

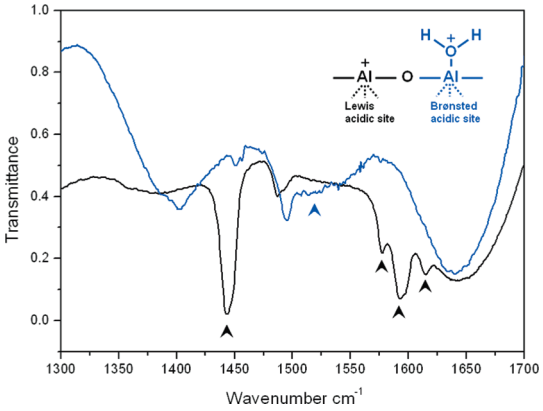

Figure 6. FTIR spectra of pyridine adsorbed on alumina support heat treated in Ar and H_2 (black) and in Ar and H_2 in the presence of water with similar conditions to those in ref 38 (blue). The bands at 1440, 1575, 1590, and 1620 cm^{-1} are a clear signature of Lewis acidic sites present on the surface of alumina materials. These sites are transformed into Brønsted acidic sites at 750 °C by the presence of water. In addition to the disappearance of the bands representative of the Lewis acidic sites, a broad band centered at 1520 cm^{-1} confirms the presence of Brønsted acidic sites, as well as the conversion of the acidity of alumina when water molecules are present in the reactor at 750 °C.

can catalyze the oxidation of amorphous carbon by water, making the process more efficient on the nanoparticle surface than on the CNT surface. Another proposition is that water limits nanoparticle coarsening, which is known to cause a reduction of the catalytic activity. However, this reduction in coarsening cannot be responsible alone for the drastic enhancement of the CCVD process, as the maximum thickness of CNT carpet obtained in the corresponding study is limited only to 200 μm.[38] In our experiment, we obtained 200 μm thickness just using native Lewis acidic sites of as-deposited alumina support without introduction of water. Moreover, Figure 3 shows particles having the same diameter to yield CNTs with different length depending on the acid−base properties of the support. Acid properties of the support can be modified when water is introduced in the reactor at 750 °C. Lewis acidic sites can be converted into Brønsted acidic sites as shown by pyridine adsorption (Figure 6). The carpet thickness is subsequently increased to 950 μm.[39] The conversion of Lewis into Brønsted sites is most probably partial since only traces of water are introduced, which results in the simultaneous existence of both types of acidic sites on the surface of alumina support during the growth of CNTs. However, the presence of Brønsted acidic sites is proposed to improve the dehydrogenation and aromatization rate of hydrocarbons adsorbed on the surface of the support as observed in the cracking reaction of paraffin and olefin.[40] Consequently, the enhancement of the CNT growth in the presence of water can be attributed to the increased catalyst selectivity for reactions yielding CNT precursors with a high degree of

aromatization. However, our experiments show that the modification of the selectivity is more efficient over a basic alumina support.

In conclusion, we have reported a simple and highly efficient catalyst activation process for the CCVD growth of CNTs based on a chemical treatment of the catalytic particles' support. The observed enhancement and reduction of the catalyst activity when treated with basic and acidic solution, respectively, illustrate the influence of the catalyst support properties on the hydrocarbon chemistry on its surface. While basic sites catalyze the aromatization and reduce the complexity of the hydrocarbon fragments adsorbed on the support surface, acidic sites are quickly poisoned by the generation of large and unsaturated hydrocarbons. In the new mechanism, CNT growth stems on the surface of the support and continues on the nanoparticles where fragments are assembled to build the CNT structure. The kinetic of the CNT growth depends dramatically on the structure of the hydrocarbons generated on the support surface and is enhanced when fragments with a high degree of aromatization and low complexity are formed. On the basis of these results, the role of water in the super growth CVD process is discussed. Water molecules modify the acidity of the support surface (from Lewis to Brønsted), which influences the hydrocarbon chemistry in favor of the production of aromatic precursors of CNTs. However, basic supports are more selective than supports with Brønsted acidic sites. Finally, we mention that MgO, a strongly basic oxide, was the first oxide-based substrate used for the growth of graphene materials,[41] corroborating further the importance of basic substrates in the synthesis of graphitic nanomaterials by CCVD.

METHODS

Catalyst Deposition. A Si wafer with 500 nm of thermal oxide was used as substrate. Ten nanometer thick film of alumina and titania was deposited by e-beam evaporation and RF sputtering, respectively. Al_2O_3 (99.99%) and TiO_2 (99.5%) were purchased from Umicore. Fe thin films were subsequently deposited also by e-beam evaporation. Fe_2Co thin films were grown by the RF magnetron sputtering technique from a Fe_2CoO_4 pellet. The deposition was carried out in a vacuum chamber at a pressure of 6×10^{-3} Torr. High purity argon (99.9999%) was used as the sputtering gas. All Fe_2Co depositions were done at an RF power of 35 W. During the Fe and Fe_2Co film deposition, the substrate was kept at room temperature.

Chemical Treatment of the Catalyst. Acid−base properties of the Al_2O_3 and TiO_2 buffer layer were modified by chemical treatment. The substrates (corresponding to about 10 cm^2 of the Si wafer) were immersed into 100 mL solutions with a pH adjusted between 4 and 12 by addition of HCl or NH_4OH purchased from Sigma-Aldrich. The chemical treatments were carried out at 60 °C for 12 h. The samples were subsequently dried and rinsed by immersing the catalyst in distilled water for a few seconds.

Carbon Nanotube Growth. CNT carpets were grown by catalytic chemical vapor deposition. As obtained after chemical treatment, substrates placed on a quartz boat are introduced into a quartz tube furnace heated at 750 °C. In a standard growth process performed at the same temperature, the samples are first kept in Ar (80 sccm, purity 99.9999%) and H_2 (80 sccm, purity 99.995%) for 10 min, after which the growth proceeds for 30 min. After the growth, the reactor is cleaned by an additional 10 min treatment under Ar (80 sccm). The samples are then cooled to room temperature under Ar by pushing out the quartz boat from the heated zone. When ethylene is used as the carbon source in the CVD process, the atmosphere is composed of ethylene (50−200 sccm, purity 99.95%), Ar, and H_2 (80 sccm, purity 99.995%). In the case of oxidative dehydrogenation chemistry, an equimolar mixture of acetylene C_2H_2 (99.6%) and CO_2 (99.998%) is introduced into a horizontally mounted quartz tube furnace at 750 °C. The growth proceeds for 30 min by introducing simultaneously acetylene (16 sccm), CO_2 (16 sccm), and Ar (750 sccm). After the growth, the reactor is cleaned by a 10 min treatment under Ar (750 sccm), and the samples are cooled to room temperature by a similar process described above.

Fourier Transformed Infrared (FTIR) of Pyridine. Pyridine adsorption is performed on alumina previously heat treated at 750 °C for 10 min in a water-free atmosphere under Ar (80 sccm) and H_2 (80 sccm). Pyridine adsorption is performed also on alumina treated in water assisted conditions (see ref 38). In addition to Ar (80 sccm) and H_2 (80 sccm), H_2O is introduced for 30 min by bubbling argon (20 sccm) in liquid water kept at a constant temperature of 19 °C. The atmosphere is dried at 750 °C by flushing the quartz chamber with pure argon. Samples are subsequently cooled to room temperature under dry Ar. Vapors of pyridine are then introduced into the chamber at room temperature. The samples are not exposed to air between the heat treatment and the pyridine adsorption. Samples were analyzed by FTIR spectroscopy using a PerkinElmer FTIR Spectrum GX spectrometer. The spectrometer was flushed with dry nitrogen before and during the measurements. For each spectrum, 16 scans were taken at room temperature from 3000 to 600 cm^{-1}.

Acknowledgment. We acknowledge G. Margaritondo and A. M. Ionescu for their help and fruitful discussions. We thank Vincent Laporte and Nicolas Xanthopoulos for the XPS analysis and the Centre Interdisciplinaire de Microscopie Electronique (CIME) for access to the electron microscopes and technical support. We acknowledge the Swiss National Science Foundation for funding the project CABTURES within its Nano Tera program. The work done by R.S, J.C.A., and D.A. was founded by the European project VIACARBON. The work was also financially supported by the European project MULTIPLAT. The work done by P.R.R. was supported by the Swiss National Science Foundation and by the Center for Biomolecular Imaging (CIBM), in turn supported by the Louis-Jeantet and Leenaards foundations. J.W.S. thanks the Belgian Hercules Stichting for their support in HER/08/25 and the K.U. Leuven for the support in STRT1/08/025 as well as GOA/10/004.

Supporting Information Available: Characterization of the supported catalyst by AFM, ESR, FTIR, XPS, characterization of carbon nanotubes by Raman scattering spectroscopy, TEM, and SEM. This material is available free of charge *via* the Internet at http://pubs.acs.org.

REFERENCES AND NOTES

1. Nessim, G. D. Properties, Synthesis, and Growth Mechanisms of Carbon Nanotubes with Special Focus on Thermal Chemical Vapor Deposition. *Nanoscale* **2010**, *2*, 1306–1323.
2. Kumar, M.; Ando, Y. Chemical Vapor Deposition of Carbon Nanotubes: A Review on Growth Mechanism and Mass Production. *J. Nanosci. Nanotechnol.* **2010**, *10*, 3739–3758.

3. MacKenzie, K. J.; Dunens, O. M.; Harris, A. T. An Updated Review of Synthesis Parameters and Growth Mechanisms for Carbon Nanotubes in Fluidized Beds. *Ind. Eng. Chem. Res.* **2010**, *49*, 5323–5338.
4. Magrez, A.; Seo, J. W.; Smajda, R.; Mionic, M.; Forró, L. Catalytic CVD Synthesis of Carbon Nanotubes: Towards High Yield and Low Temperature Growth. *Materials* **2010**, *3*, 4428–4445.
5. Harutyunyan, A. R. The Catalyst for Growing Single-Walled Carbon Nanotubes by Catalytic Chemical Vapor Deposition Method. *J. Nanosci. Nanotechnol.* **2009**, *9*, 2480–2495.
6. Takagi, D.; Homma, Y.; Hibino, H.; Suzuki, S.; Kobayashi, Y. Single-Walled Carbon Nanotube Growth from Highly Activated Metal Nanoparticles. *Nano Lett.* **2006**, *6*, 2642–2645.
7. Takagi, D.; Hibino, H.; Suzuki, S.; Kobayashi, Y.; Homma, Y. Carbon Nanotube Growth from Semiconductor Nanoparticles. *Nano Lett.* **2007**, *7*, 2272–2275.
8. Zhou, W.; Han, Z.; Wang, J.; Zhang, Y.; Jin, Z.; Sun, X.; Zhang, Y.; Yan, C.; Li, Y. Copper Catalyzing Growth of Single-Walled Carbon Nanotubes on Substrates. *Nano Lett.* **2006**, *6*, 2987–2990.
9. Liu, B. L.; Ren, W.; Gao, L.; Li, S.; Pei, S.; Liu, C.; Jiang, C.; Cheng, H. M. Metal-Catalyst-Free Growth of Single-Walled Carbon Nanotubes. *J. Am. Chem. Soc.* **2009**, *131*, 2082–2083.
10. Huang, S. M.; Cai, Q.; Chen, J.; Qian, Y.; Zhang, L. Metal-Catalyst-Free Growth of Single-Walled Carbon Nanotubes on Substrates. *J. Am. Chem. Soc.* **2009**, *131*, 2094–2095.
11. Steiner, S. A.; Baumann, T. F.; Bayer, B. C.; Blume, R.; Worsley, M. A.; Moberly Chan, W. J.; Shaw, E. L.; Schlogl, R.; Hart, A. J.; Hofmann, S.; *et al.* Nanoscale Zirconia as a Nonmetallic Catalyst for Graphitization of Carbon and Growth of Single- and Multiwall Carbon Nanotubes. *J. Am. Chem. Soc.* **2009**, *131*, 12144–12154.
12. Cantoro, M.; Hofmann, S.; Pisana, S.; Scardaci, V.; Parvez, A.; Ducati, C.; Ferrari, A. C.; Blackburn, A. M.; Wang, K. Y.; Robertson, J. Catalytic Chemical Vapor Deposition of Single-Wall Carbon Nanotubes at Low Temperatures. *Nano Lett.* **2006**, *6*, 1107–1112.
13. Magrez, A.; Seo, J. W.; Smajda, R.; Korbely, R.; Andresen, J. C.; Mionic, M.; Casimirius, S.; Forró, L. Low Temperature, Highly Efficient Growth of Carbon Nanotubes on Functional Materials by an Oxidative Dehydrogenation Reaction. *ACS Nano* **2010**, *4*, 3702–3708.
14. Magrez, A.; Seo, J. W.; Kuznetsov, V. L.; Forró, L. Evidence of an Equimolar $C_2H_2-CO_2$ Reaction in the Synthesis of Carbon Nanotubes. *Angew. Chem., Int. Ed.* **2007**, *46*, 441–444.
15. Lee, D. H.; Lee, W. J.; Kim, S. O. Highly Efficient Vertical Growth of Wall-Number-Selected, N-Doped Carbon Nanotube Arrays. *Nano Lett.* **2009**, *9*, 1427–1432.
16. Hata, K.; Futaba, D. N.; Mizuno, K.; Namai, T.; Yumura, M.; Iijima, S. Water-Assisted Highly Efficient Synthesis of Impurity-Free Single-Walled Carbon Nanotubes. *Science* **2004**, *306*, 1362–1364.
17. Zhang, G.; Mann, D.; Zhang, L.; Javey, A.; Li, Y.; Yenilmez, E.; Wang, Q.; McVittie, J. P.; Nishi, Y.; Gibbons, J.; Dai, H. Ultra-High-Yield Growth of Vertical Single-Walled Carbon Nanotubes: Hidden Roles of Hydrogen and Oxygen. *Proc. Natl. Acad. Sci. U.S.A.* **2005**, *102*, 16141–16145.
18. Nasibulin, A. G.; Brown, D. P.; Queipo, P.; Gonzalez, D.; Jiang, H.; Kauppinen, E. I. An Essential Role of CO_2 and H_2O during Single-Walled CNT Synthesis from Carbon Monoxide. *Chem. Phys. Lett.* **2006**, *417*, 179–184.
19. Dupuis, A. C. The Catalyst in the CCVD of Carbon Nanotubes: A Review. *Prog. Mater. Sci.* **2005**, *50*, 929–961.
20. Eres, G.; Rouleau, C. M.; Yoon, M.; Puretzky, A. A.; Jackson, J. J.; Geohegan, D. B. Model for Self-Assembly of Carbon Nanotubes from Acetylene Based on Real-Time Studies of Vertically Aligned Growth Kinetics. *J. Phys. Chem. C* **2009**, *113*, 15484–15491.
21. Eres, G.; Kinkhabwala, A. A.; Cui, H.; Geohegan, D. B.; Puretzky, A. A.; Lowndes, D. H. Molecular Beam-Controlled Nucleation and Growth of Vertically Aligned Single-Wall Carbon Nanotube Arrays. *J. Phys. Chem. B* **2005**, *109*, 16684–16694.
22. Yao, Y.; Feng, C.; Zhang, J.; Liu, Z. Cloning of Single-Walled Carbon Nanotubes *via* Open-End Growth Mechanism. *Nano Lett.* **2009**, *9*, 1673–1677.
23. Tanabe, K.; Misono, M.; Ono, Y.; Hattori, H. *New Solid Acids and Bases: Their Catalytic Properties*; Elsevier: Amsterdam, 1989.
24. Yamada, T.; Namai, T.; Hata, K.; Futaba, D. N.; Mizuno, K.; Fan, J.; Yudasaka, M.; Yumura, M.; Iijima, S. Size-Selective Growth of Double-Walled Carbon Nanotube Forests from Engineered Iron Catalysts. *Nat. Nanotechnol.* **2006**, *1*, 131–136.
25. Hayamizu, Y.; Yamada, T.; Mizuno, K.; Davis, R. C.; Futaba, D. N.; Yumura, M.; Hata, K. Integrated Three-Dimensional Microelectromechanical Devices from Processable Carbon Nanotube Wafers. *Nat. Nanotechnol.* **2008**, *3*, 289–294.
26. Amama, P. B.; Pint, C. L.; Kim, S. M.; McJilton, L.; Eyink, K. G.; Stach, E. A.; Hauge, R. H.; Maruyama, B. Influence of Alumina Type on the Evolution and Activity of Alumina-Supported Fe Catalysts in Single-Walled Carbon Nanotube Carpet Growth. *ACS Nano* **2010**, *4*, 895–904.
27. Kosmulski, M. *Chemical Properties of Material Surfaces*; Marcel Dekker: New York, 2001.
28. Pines, H.; Stalick, W. M. *Base-Catalyzed Reactions of Hydrocarbon and Related Compounds*; Academic Press: New York, 1977.
29. Ciuparu, D.; Ensuque, A.; Bozon-Verduraz, F. Pd Catalysts Supported on MgO, ZrO_2 or $MgO-ZrO_2$: Preparation, Characterisation and Study in Hexane Conversion. *Appl. Catal., A* **2007**, *326*, 130–142 and references therein.
30. Pines, H. *The Chemistry of Catalytic Hydrocarbon Conversions*: Academic Press: New York, 1981.
31. Davis, B. H.; Hettinger, W. P. *Heterogeneous Catalysis*. ACS Symposium Series; American Chemical Society: Washington, D.C., 1983.
32. DiLeo, R. A.; Landi, B. J.; Raffaelle, R. P. Purity Assessment of Multiwalled Carbon Nanotubes by Raman Spectroscopy. *J. Appl. Phys.* **2007**, *101*, 064307.
33. Meshot, E. R.; Plata, D. L.; Tawfick, S.; Zhang, Y.; Verploegen, E. A.; Hart, A. J. Engineering Vertically Aligned Carbon Nanotube Growth by Decoupled Thermal Treatment of Precursor and Catalyst. *ACS Nano* **2009**, *3*, 2477–2486.
34. Plata, D. L.; Meshot, E. R.; Reddy, C. M.; Hart, A. J.; Gschwend, P. M. Multiple Alkynes React with Ethylene To Enhance Carbon Nanotube Synthesis, Suggesting a Polymerisation-like Formation Mechanism. *ACS Nano* **2010**, *4*, 7185–7192.
35. In the Raman spectrum of CNTs of ref 33 produced at 750 °C with an optimum preheat treatment of the carbon source at 1020 °C, the ratio I_D/I_G is about 1.1. The length of the CNTs is about 750 μm, and the catalyst lifetime is limited to about 6 min. When the catalyst is chemically pretreated with a basic solution, the I_D/I_G ratio is reduced to 0.7, the length of the CNTs is about 1.35 mm, and the catalyst lifetime is extended to about 30 min. The growth conditions (including the nature and the flux of the gas, the thickness of the Fe and Al_2O_3 films) are identical in both sets of experiments.
36. Yamada, T.; Maigne, A.; Yudasaka, M.; Mizuno, K.; Futaba, D. N.; Yumura, M.; Iijima, S.; Hata, K. Revealing the Secret of Water-Assisted Carbon Nanotube Synthesis by Microscopic Observation of the Interaction of Water on the Catalysts. *Nano Lett.* **2008**, *8*, 4288–4292.
37. Yasuda, T; Hiraoka, T.; Futaba, D. N.; Yamada, T.; Yumura, M.; Hata, K. Existence and Kinetics of Graphitic Carbonaceous Impurities in Carbon Nanotube Forests To Assess the Absolute Purity. *Nano Lett.* **2009**, *9*, 769–773.
38. Amama, P. B.; Pint, C.; McJilton, L.; Kim, S. M.; Stach, E. A.; Murray, P. T.; Hauge, R. H.; Mayurama, B. Role of Water in Super Growth of Single-Walled Carbon Nanotube Carpets. *Nano Lett.* **2009**, *9*, 44–49.
39. Smajda, R.; Andresen, J. C.; Duchamp, M.; Meunier, R.; Casimirius, S.; Hernadi, K.; Forró, L.; Magrez, A. Synthesis

and Mechanical Properties of Carbon Nanotubes Produced by the Water Assisted CVD Process. *Phys. Status Solidi B* **2009**, *246*, 2457–2460.
40. Le Van Mao, R.; Dufresne, L. A.; Yao, J.; Yu, Y. Effects of the Nature of Coke on the Acidity and Stability of the Hybrid Catalyst Used in the Aromatization of Ethylene and *n*-Butane. *Appl. Catal., A* **1997**, *164*, 81–89.
41. Rummeli, M. H.; Bachmatiuk, A.; Scott, A.; Borrnert, F.; Warner, J. H.; Hoffman, V.; Lin, J. H.; Cuniberti, G.; Buchner, B. Direct Low-Temperature Nanographene CVD Synthesis over a Dielectric Insulator. *ACS Nano* **2010**, *4*, 4206–4210.